Space: Science & Technology
A SCIENCE PARTNER JOURNAL

RESEARCH ARTICLE

Catastrophic Failure Assessment of Sealed Cabin for Ultra large Manned Spacecraft in M/OD Environment

Jiangkai Wu[1,2], Zengyao Han[1,3], Runqiang Chi[1*], Shigui Zheng[2], and Yong Zhang[2]

[1]Harbin Institute of Technology, Harbin, 150001 Heilongjiang Province, China. [2]Beijing Institute of Spacecraft System Engineering, Beijing 100094, China. [3]China Satellite Network Group Co. Ltd., Xiongan New Area 071700, China.

*Address correspondence to: chirq@hit.edu.cn

Citation: Wu J, Han Z, Chi R, Zheng S, Zhang Y. Catastrophic Failure Assessment of Sealed Cabin for Ultra large Manned Spacecraft in M/OD Environment. *Space Sci. Technol.* 2023;3:Article 0022. https://doi.org/10.34133/space.0022

Submitted 2 October 2022
Accepted 19 February 2023
Published 30 March 2023

Copyright © 2023 Jiangkai Wu et al. Exclusive licensee Beijing Institute of Technology Press. No claim to original U.S. Government Works. Distributed under a Creative Commons Attribution License (CC BY 4.0).

Hypervelocity impacts of Micrometeoroid and Orbital Debris (M/OD) may lead to catastrophic failure of long-term flight manned spacecraft in orbit. Risk assessment for manned spacecraft in M/OD environment is of great significance for the safety of human space missions. For typical catastrophic failure modes of manned spacecraft such as gas-leakage-induced astronaut hypoxia, sealed cabin fracture, and spacecraft breakup, catastrophic failure assessment method using critical perforation diameters and critical crack lengths of sealed cabins and critical fragment size of spacecraft breakup as failure criteria are proposed. In addition, corresponding modules of catastrophic failure assessment were developed and integrated with Meteoroid and Orbital Debris Assessment and Optimization System Tools, providing an effective assessment tool for researching on the safety of manned spacecraft. On the basis of which, catastrophic failure evaluation of sealed cabin for a specific ultralarge manned spacecraft in the M/OD environment was conducted, providing references for on-orbit mission safety evaluation.

Downloaded from https://spj.science.org on October 20, 2023

Introduction

Hypervelocity impacts of Micrometeoroid and Orbital Debris (M/OD) seriously threaten the safety of manned spacecraft and astronauts in orbit. At present, M/OD above 10 cm, which can be monitored and predicted in advance, it can usually be avoided by orbital maneuver, and the collision probability is very low. As for the small-size M/OD, because of the difficulty of monitoring, it is the main impact threat, as well as the main object of impact risk assessment and protection design of manned spacecraft. The probability of no penetration (PNP) of the sealed cabin under M/OD impact is usually used as the method to assess the probability of no failure of the system in manned space missions [1,2]. That is, it is conservatively considered that the penetration of the sealed cabin of manned spacecraft will directly cause spacecraft failure or astronaut casualties. One of the direct consequences of this method is that the shield is overdesigned. However, for ultralarge manned spacecraft such as the International Space Station (ISS), even if the sealed cabin is penetrated by debris, the penetration will not necessarily cause spacecraft failure or astronauts casualties. They are also closely related to factors like the pressure regime in the sealed cabin and the tolerance of the astronauts. In addition, such an ultralarge manned spacecraft is generally assembled by several mutually isolated and independent sealed cabin modules, which can be connected by mutually independent hatches. So even if one sealed cabin module is penetrated by debris, catastrophic failure can still be avoided through emergency flight plans such as on-orbit emergency plugging or repair, transfer, evacuation, or escape of the astronauts. In addition, researchers have also developed that self-healing polymeric materials for deployable sealed cabins, which can be repaired by presetting hollow fiber tubes or microcapsules in the bulkhead structure, repair autonomously after accidental damages caused by collision with M/OD. After the structural perforated, the fiber tubes or microcapsules will break, the internal repair agent will be automatically filled to the perforation position, and the repair will be realized under the combined action of the pressure difference between inside and outside the cabins and the air flow. Unfortunately, this technology is not yet mature and has not been applied in space, and application objects are limited to inflatable structures [3].

For the reason, researchers proposed using the probability of no catastrophic failure (PNCF) to quantitatively evaluate catastrophic failures of spacecraft in M/OD environment. PNCF is expressed by Eqs. 1 and 2 [4].

$$\mathrm{PNCF} = \mathrm{PNP}^R \tag{1}$$

$$\mathrm{PNCF} = (1-\mathrm{PP})^R \tag{2}$$

where PP represents the probability of penetration, PP = 1 − PNP, and R is the evaluation factor of a certain failure mode of spacecraft, indicating the proportion of probability of failure of the

spacecraft in its PP. The probability of one catastrophic failure is expressed as PCF = 1 − PNCF.

To improve the accuracy of assessing the safety and survivability of manned spacecraft (e.g., ISS) and astronauts, the National Aeronautics and Space Administration (NASA) successfully developed the Manned Spacecraft Crew Survivability (MSCSurv) computer code in 1992. Moreover, it established models for the 6 catastrophic failure modes of pressurized cabin fracture, critical equipment loss, gas-leakage-induced loss of attitude control, gas-leakage-induced astronaut hypoxia, fatal injuries of the astronauts, and failure of the astronauts to escape because of depressurization of critical cabin segments (Fig. 1). In the MSCSurv, PNCF was used to quantitatively assess on-orbit survivability of ISS under M/OD impact. Compared with PNP, PNCF characterizes a lower probability of spacecraft failure and crew casualties, allowing designers to consume fewer resources in debris protection design to ensure the safety of spacecraft and the astronauts [5].

At present, the PNP of sealed cabins was still used as the method for assessing the probability of one catastrophic failure in the design of manned spacecraft in China. This leads to inaccurate risk assessment of catastrophic failures of manned spacecraft in M/OD environment. Therefore, in the context of on-orbit safety assessment of an ultralarge manned spacecraft, critical perforation diameters and critical crack lengths (CCLs) of sealed cabins in response to typical catastrophic failure modes were studied, including gas-leakage-induced astronaut hypoxia, sealed cabin fracture, and spacecraft breakup. On this basis, a failure assessment module was developed to improve the Meteoroid and Orbital Debris Assessment and Optimization System Tools (MODAOST) [6], which developed by the China Academy of Space Technology, provides more effective assessment tools for studying catastrophic failures of ultralarge manned spacecraft in M/OD environment. Moreover, to solve perforation diameters and crack lengths of the sealed cabin of a specific ultralarge manned spacecraft, ballistic limit equations and perforation and crack equations suitable for stuffed Whipple shields were established through revision with the data of impact tests on the ground. Finally, we quantitatively assessed the catastrophic failures of the ultralarge manned spacecraft in M/OD environment with its design parameters like the flight orbit, attitude, and configuration, thus providing reference for on-orbit safety assessment of spacecraft.

Typical Catastrophic Failures of Manned Spacecraft in an M/OD Environment

Sealed cabins provide astronauts' places for long-term on-orbit living and working. The perforation of the sealed cabin under M/OD impact can induce gas leakage in the cabin and then lead to cabin depressurization and astronaut hypoxia. Unstable propagation of cabin cracks and sealed cabin fracture are the primary factors inducing catastrophic failures of spacecraft in M/OD environment [5].

Astronaut hypoxia

Oxygen partial pressure and total pressure are important indicators for manned spacecraft to ensure astronauts work and live on-orbit. After the sealed cabin was perforated, the cabin rapidly changes to a low-pressure and hypoxic environment. Low pressure will cause barotrauma to the astronauts, while hypoxia will cause the astronauts to suffer acute hypoxia and then become unconscious or suffocate. Both can seriously threaten the life of astronauts [7]. For the astronaut casualty mode caused by low-pressure or hypoxic environment, hereinafter collectively referred to as astronaut hypoxic failure mode.

Failure criterion

After the perforation of the sealed cabin of the manned spacecraft, astronauts should urgently complete the emergency plugging and maintenance of the cabin or evacuate and escape according to the predetermined plan. The critical escape time

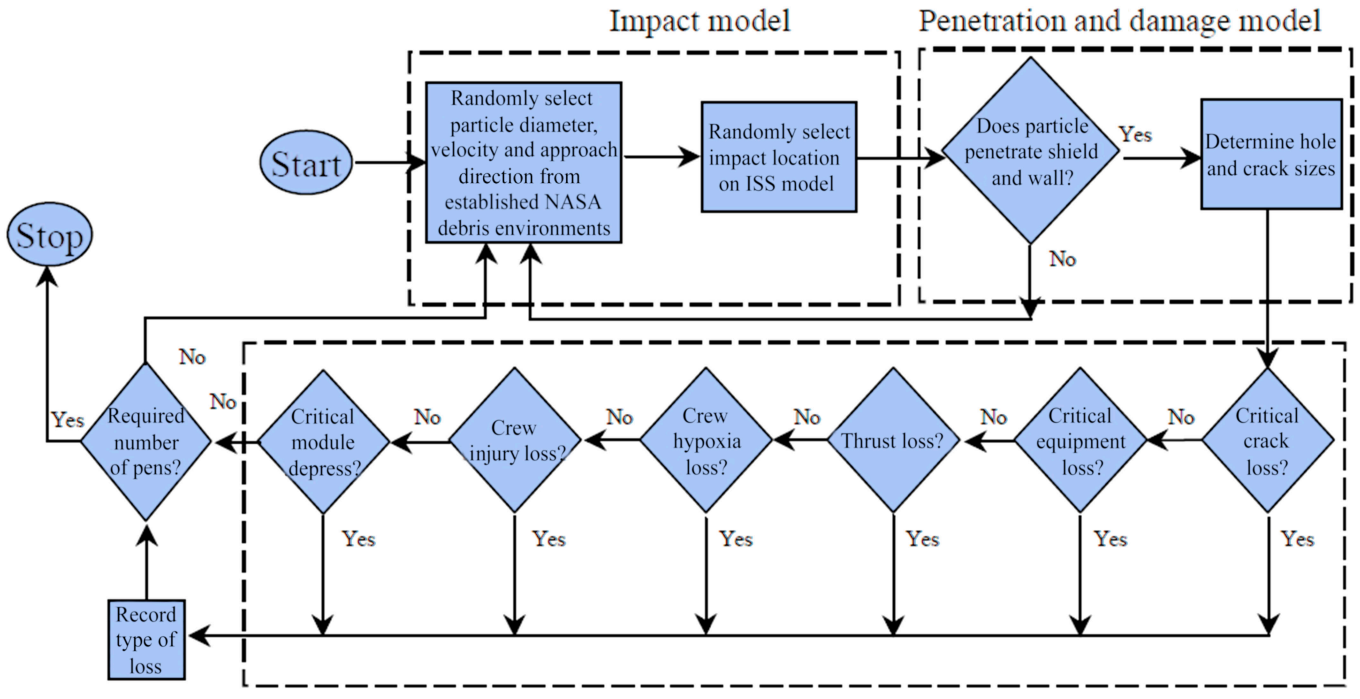

Fig. 1. Flow chart of MSCSurv.

Downloaded from https://spj.science.org on October 20, 2023

T_{CE} is defined as the shortest time from the leakage of the cabin to the completion of emergency evacuation and escape or plugging repair. The critical total pressure P_{TE} and critical oxygen partial pressure are defined as the lowest total pressure and oxygen partial pressure support astronauts to escape. In case of emergencies such as perforated gas leak that occurs in the cabin, the gas pressure control system in the sealed cabin should keep the total pressure not lower than P_{TE}, the oxygen partial pressure not lower than P_{O^2E}, and duration not less than the critical escape time T_{CE} to support the astronauts in emergency on-orbit plugging or evacuation.

Because of the huge quantity of M/OD, the calculation of perforation hole diameter for each M/OD impact particle and the corresponding total pressure and oxygen partial pressure after T_{CE} is very large, which results in low evaluation efficiency. We define D_{hE} as the critical perforation diameter that causes astronaut hypoxia failure. When the perforation diameter D_h of the sealed cabin is smaller than D_{hE}, total pressure and oxygen partial pressure at T_{CE} are higher than P_{TE} and P_{O^2E}, respectively. As a result, the astronaut hypoxia failure will not occur. In the case of D_h greater than D_{hE}, the total pressure is lower than P_{TE}, or oxygen partial pressure is lower than P_{O^2E} at T_{CE}. Then, astronaut hypoxia failure happens.

Therefore, according to the given parameters of the sealed cabin, such as shield structure, cabin volume, initial total pressure, initial oxygen partial pressure, initial temperature, and gas supply rate, this paper solves the critical perforation diameter D_{hE} that satisfies the emergency escape of astronauts. By which, converting the astronaut hypoxia failure criterion from whether total pressure and oxygen partial pressure at T_{CE} meet requirements of P_{TE} and P_{O^2E}, respectively, to whether perforation diameter under M/OD impact is smaller than D_{hE}.

Analysis of critical perforation diameter

It is supposed that a hole with diameter of D_h is produced on the wall of a sealed cabin after M/OD impact, as shown in Fig. 2.

To simplify the model for gas leakage analysis, it is assumed that the air in the sealed cabin is ideal gas; gas leakage velocity is perpendicular to the cross-sections of the hole; temperature, velocity, pressure, and density of gas remain unchanged in the leakage direction. In addition, considering the initial pressure and flow of air in the cabin is higher than outer space, the duration of leakage is short, the heat exchange between the leaking gas and the cabin is ignored, the gas leakage process is approximated as an adiabatic isentropic flow, and a one-dimensional Laval nozzle model was used to describe gas leakage at the through hole on the cabin wall.

The gas flow parameters at the perforation hole depend on the ratio of the outer pressure P_o ($P_o = 0$ Pa for a large manned spacecraft in orbit) and the inner gas pressure P_i of the cabin. Thus, when P_o/P_i is less than 0.5283, the velocity of gas leakage reaches the local velocity of sound (that is, $M_a = 1$). According to the gas continuity equation, jet velocity and leaking gas mass flow at the perforation of the sealed cabin are obtained as follows [8]:

$$v_l = \sqrt{\gamma P_l \rho_l} \tag{3}$$

$$\dot{m}_l = \pi D_h^2 \rho_l v_l / 4 \tag{4}$$

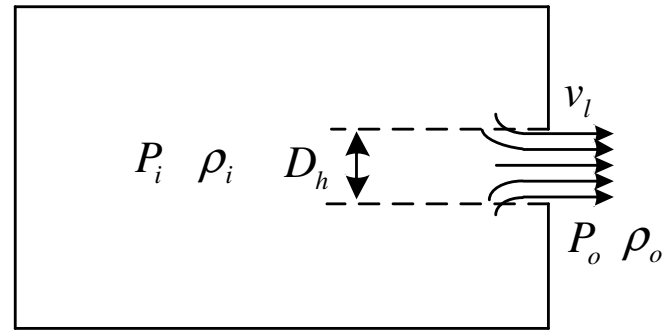

Fig. 2. Schematic diagram of Gas leakage in sealed cabin penetrated by M/OD.

where v_l P_l and ρ_l represent flow velocity, pressure, and density of gas at the perforation, respectively; $\dot{m}_l$ is gas mass flow at the perforation; and γ is an adiabatic expansion coefficient (for air, $\gamma = 1.4$).

It is supposed that the oxygen consumption of the astronauts and the normal gas supply rate in the cabin are constant during gas leakage. Without considering internal gas flow and normal gas outflow of the sealed cabin was ignored, according to the assumption of adiabatic isentropic expansion of ideal gas, the gas pressure and density at the perforated hole are obtained by Eqs. 5 and 6:

$$P_l = P_i \left(\frac{2}{\gamma + 1} \right)^{\gamma/\gamma - 1} \tag{5}$$

$$\rho_l = \rho_i \left(\frac{2}{\gamma + 1} \right)^{1/\gamma - 1} \tag{6}$$

Substituting them into Eq. (4) yields gas mass flow at the perforation:

$$\dot{m}_l = \frac{\pi D_h^2}{4} \sqrt{\gamma \left(\frac{2}{\gamma + 1} \right)^{\gamma + 1/\gamma - 1} P_i \rho_i} \tag{7}$$

where P_i and ρ_i represent gas pressure and density in the sealed cabin during the leakage, respectively. They were calculated by Eq. 8 according to the assumption of adiabatic isentropic expansion.

$$P_i = \rho_i^{\gamma} \frac{P_{i0}}{\rho_{i0}^{\gamma}} \tag{8}$$

where P_{i0} and ρ_{i0} represent the initial pressure and density of gas in the sealed cabin, respectively. In the case of a fixed volume V_{cabin} of the sealed cabin, P_{i0} and ρ_{i0} as well as P_i and ρ_i are all satisfied thermal equations of state of an ideal gas. According to Eqs. 3 to 8, we can obtain variations in the internal pressure of the sealed cabin at a perforation diameter of D_h and the critical perforation diameter D_{hE} of the cabin at a given T_{CE}.

Example

The case in the study of Jian et al. [9] was selected for analysis. The basic parameters of the sealed cabin are as follows: a cabin volume of 36 m^3, an initial temperature of 21 °C, an initial total pressure of 97.0 kPa, an initial oxygen partial pressure of

Downloaded from https://spj.science.org on October 20, 2023

20.6 kPa, an external ambient pressure of 1.01×10^{-5} Pa, and respective supply rates of 12 and 18 g/s for oxygen and nitrogen cylinders in emergency. The average oxygen consumption rate of the 3 astronauts is 0.01 g/s per person. When the oxygen partial pressure drops to 20.0 kPa, the oxygen supply component functions, and when the total pressure drops to 87.0 kPa, the nitrogen supply component starts to work [9]. To satisfy the survival requirement, the total pressure P_{TE} during on-orbit emergency leakage plugging or evacuation should be 70 kPa, and the oxygen partial pressure P_{O^2E} is 14 kPa. With the above parameters, the variations in oxygen partial pressure and total pressure in the sealed cabin are shown at different perforation diameters (Figs. 3 and 4). It can be seen that greater perforation diameters result in faster gas leakage of the sealed cabin and shorter time available for astronauts to escape.

The time for ensuring emergency leakage plugging or evacuation of the astronauts in the sealed cabin was assumed to 1,200 s. Then, under the given gas supply rate, the critical perforation diameter for no catastrophic failures of the sealed cabin is calculated as 1.54 cm by Eqs. 5 to 8. In other words, when the perforation diameter is more than 1.54 cm, astronaut hypoxia failure will occur.

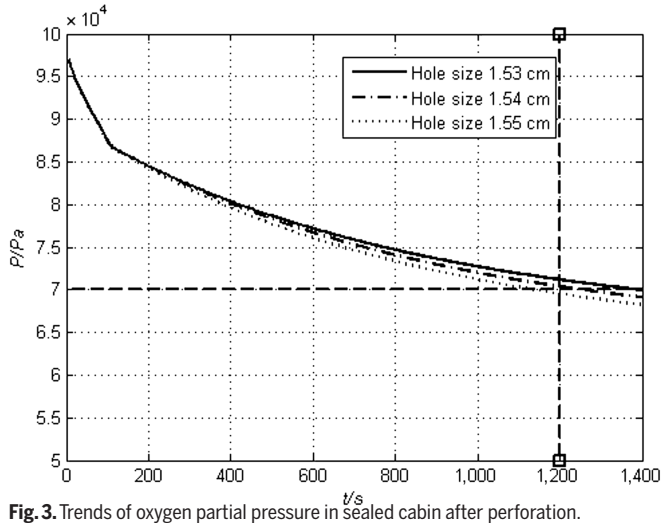

Fig. 3. Trends of oxygen partial pressure in sealed cabin after perforation.

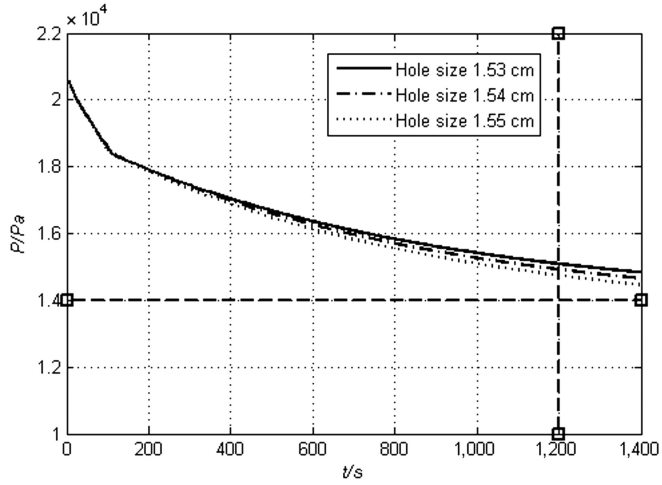

Fig. 4. Trends of total pressure in sealed cabin after perforation.

Sealed cabin fracture

After the sealed cabin of manned spacecraft was hit by M/OD, in addition to through holes, cracks of different lengths may also occur in the cabin. Under the internal pressure of the sealed cabin, unstable propagation of the cracks will take place, thereby resulting in fragmentation or cracking of the cabin.

Failure criterion

Under the internal pressure of the sealed cabin, cracks induced by M/OD impact may propagate or expand, resulting in depressurization and then catastrophic failure of the cabin. When the stress intensity factor (SIF) at the tip of a crack on the cabin wall is equal to the fracture toughness of the wall material, the corresponding crack length is defined as the CCL of the sealed cabin. Under M/OD impact, if the crack length is greater than the CCL, SIF at the crack tip exceeds the fracture toughness of the material and, thus, the sealed cabin fractures. When the crack length is shorter than CCL, the cabin would be perforated by a petal-shaped crack, which was regarded as more serious perforation failure.

Analysis of CCL

For the slender cylindrical sealed cabin structure, the circumferential stress σ_h of its cylindrical wall is about twice the axial stress σ_a, as shown in Eq. 9. Thus, it can be seen that axial cracks are more likely to appear on the wall of the sealed cabin under M/OD impact [10].

$$\sigma_h = 2\sigma_a = R_m P_c / t_w \tag{9}$$

where R_m represents the radius of the sealed cabin, P_c represents the internal pressure of the sealed cabin, and t_w represents the wall thickness of the sealed cabin.

The linear elastic fracture mechanics theory was used to analyze the SIF at the tip of a crack on the sealed cabin wall under different crack lengths and then compared with the fracture toughness of the cabin material to obtain the CCL of the sealed cabin [10]. Conservatively, the effect of wall stiffener on SIF at the crack tip is ignored. Therefore, the relationship between SIF at the tip of an axial crack on a cylindrical cabin wall and crack length, which proposed by Folias, was used in this paper, as shown in the Eq. 10 [11].

$$K_I = \frac{P_c R_m \sqrt{\pi a_0}}{t_w} \left[1 + 1.66 \left(\frac{a_0^2}{R_m t_w} \right) \right]^{\frac{1}{2}} \tag{10}$$

where K_I represents SIF at the tip of an axial crack and a_0 is half of the length of an axial crack on the cabin wall.

When the length of a crack on the sealed cabin wall is greater than CCL, unstable propagation of the crack takes place, resulting in fragmentation and cracking of the cabin.

Example

For a specific ultralarge manned spacecraft, the assumed parameters are as follows: a sealed cabin radius R_m of 205 cm, a wall thickness of 0.25 cm, an internal pressure of 1.01×10^5 Pa, and a fracture toughness of 7.08×10^7 Pa·m$^{1/2}$ for the aluminum alloy wall. On this basis, we calculate the relationship between SIF at the tip of a crack on the cabin wall and crack length using Eq. 10 (Fig. 5). The calculated CCL of the cylindrical sealed cabin is about 15.7 cm.

Downloaded from https://spj.science.org on October 20, 2023

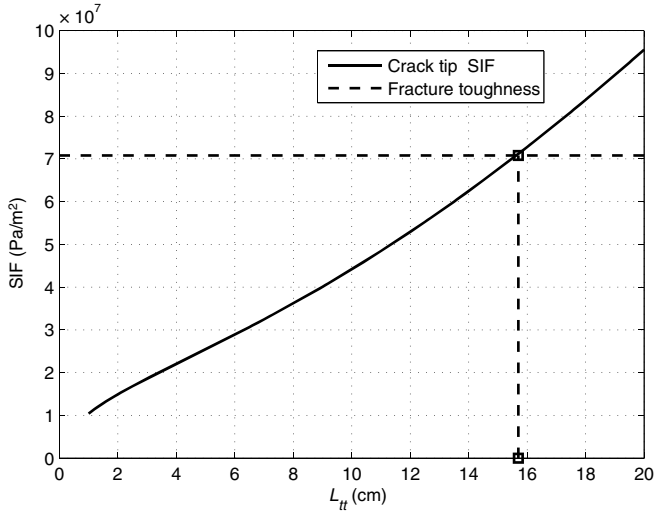

Fig. 5. Comparison of SIF at the tip of a crack on sealed cabin wall and crack length.

For this sealed cabin, a crack propagation failure will occur when an M/OD impact-induced crack is longer than 15.7 cm.

Spacecraft breakup

Spacecraft breakup is the most serious failure mode of manned spacecraft. At present, NASA's breakup threshold is widely used to judge whether a spacecraft breaks up. Specifically, if the ratio of the kinetic energy of impact debris to the mass of the spacecraft is greater than 40 J/g, then the spacecraft is considered to break up. However, this criterion is poorly applicable to the cases in which centimeter-scaled debris hits ultralarge manned spacecraft of tens or even hundreds of tons [12]. Therefore, according to Williamsen [13], the M/OD critical size criterion was used for cabin breakup failure mode assessment. When the M/OD particle impacted on the sealed cabin is larger than 3 cm in size, the spacecraft would fail to break up [13].

Perforation and Crack Equations for Stuffed Whipple Shield of Sealed Cabin

The perforation diameter and crack length of the sealed cabin wall under M/OD impact are important bases for catastrophic failure assessment under the failure modes of astronaut hypoxia and cabin fracture. Stuffed Whipple shield was used for the sealed cabin of a specific ultralarge manned spacecraft, with basalt fiber fabric and aramid fiber fabric selected as stuffing materials [1]. Figure 6 illustrates the shield [14].

Ballistic limit equations of stuffed Whipple shield

The ballistic limit equations of the stuffed Whipple shield are important bases for studying perforation equations. The current international common empirical perforation equations were developed and verified on the basis of shield ballistic limits [15,16]. To obtain more accurately ballistic limit equations of the stuffed Whipple shield, hypervelocity impact tests on 3 types of stuffed Whipple shields were completed, obtaining the ballistic limits of such shields. Figure 7 shows damage to the shield, including the bumper, the stuffing layer, and the cabin wall.

On the basis of the genetic algorithms and multiple linear regression method, the coefficients of NASA's Christiansen equation commonly used in the world were corrected, and the

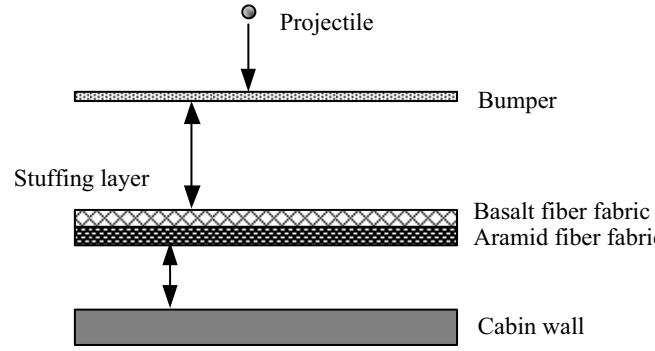

Fig. 6. Schematic diagram of stuffed Whipple shield.

ballistic limit equations suitable for the stuffed Whipple shield of a specific ultralarge manned spacecraft was obtained, as shown in Eqs. 11 to 13 [17].

In the case of $V \le 2.6/(\cos\theta)^{0.5}$

$$D_{BL} = 2.35 \times \left(0.1203 \times t_w (\sigma/275.8)^{0.5} + 0.792 \times 0.37 m_b\right) \times \rho_P^{-0.5} \times V^{-2/3} \times (\cos\theta)^{-0.75} \quad (11)$$

In the case of $V \ge 6.5/(\cos\theta)^{0.75}$

$$D_{BL} = 0.6 \times \rho_P^{-1/3} \times (\sigma/275.8)^{1/6} \times \left(t_w \rho_w\right)^{0.08} \times S^{0.575} \times V^{-1/3} \times (\cos\theta)^{-0.75} \quad (12)$$

In the case of $2.6/(\cos\theta)^{0.5} < V < 6.5/(\cos\theta)^{0.75}$

$$D_{BL} = 2.35 \times \left(2.6/(\cos\theta)^{0.5}\right)^{-2/3} \times \left(0.1203 \times t_w (\sigma/275.8)^{0.5} + 0.792 \times 0.37 m_b\right) \times \rho_P^{-0.5} \times (\cos\theta)^{-0.75} \times \frac{6.5/(\cos\theta)^{0.75} - V}{6.5/(\cos\theta)^{0.75} - 2.6/(\cos\theta)^{0.5}} + 0.6 \times \left(t_w \rho_w\right)^{0.08} \times S^{0.575} \times \left(6.5/(\cos\theta)^{0.57}\right)^{-1/3} \times \rho_P^{-1/3} \times (\sigma/275.8)^{1/6} \times (\cos\theta)^{-0.5} \times \frac{V - 2.6/(\cos\theta)^{0.5}}{6.5/(\cos\theta)^{0.75} - 2.6/(\cos\theta)^{0.5}} \quad (13)$$

In Eqs. 11 to 13, D_{BL} represents the critical projectile diameter (cm), t_w represents the thickness of the cabin wall (cm), σ represents the yield strength of the cabin wall (MPa), m_b represents the total areal density of the bumper and the stuffing layer (g/cm^2), ρ_P represents the projectile density (g/cm^3), V represents the projectile impact velocity (km/s), θ is the projectile impact angle (°), ρ_w represents the cabin wall density (g/cm^3); and S represents the distance between the bumper and the cabin wall (cm). While the rest are dimensionless ones, 2.35 (g$^{1/2}$cm$^{-3/2}$km$^{-2/3}$s$^{-2/3}$), 275.8 (MPa), 0.37 (g^{-1}cm^3), 0.6 (km$^{1/3}$s$^{-1/3}$), 0.37 (g^{-1}cm^3), 6.5 (km/s), and 2.6 (km/s) are dimensional constants.

Perforation and crack equations of stuffed Whipple shield

With the above corrected ballistic limit equations of the stuffed Whipple shield and the perforation data of impact tests, the perforation equation for region 1 of the W-S hole equation was corrected [16]. On this basis, the equations of perforation diameter and crack length on the sealed cabin were obtained, which are suitable for the stuffed Whipple shield of a specific ultralarge

Downloaded from https://spj.science.org on October 20, 2023

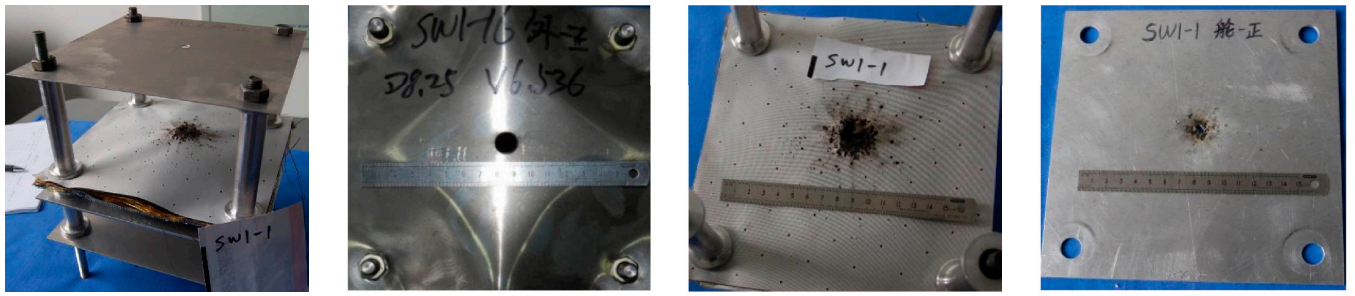

A Whole **B** Bumper **C** Stuffing layer **D** Cabin wall

Fig. 7. Impact damage characteristics of stuffed Whipple shield test piece. (A) Whole, (B) bumper, (C) stuffing layer, and (D) cabin wall.

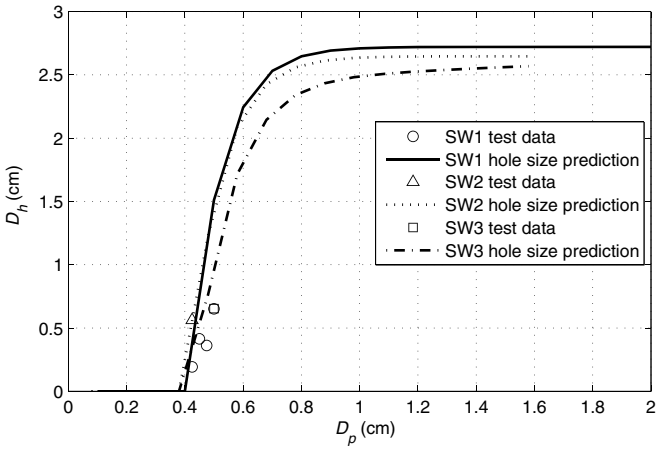

Fig. 8. Hole size prediction with modified W-S equation ($V = 3$ km/s, 0° impact angle).

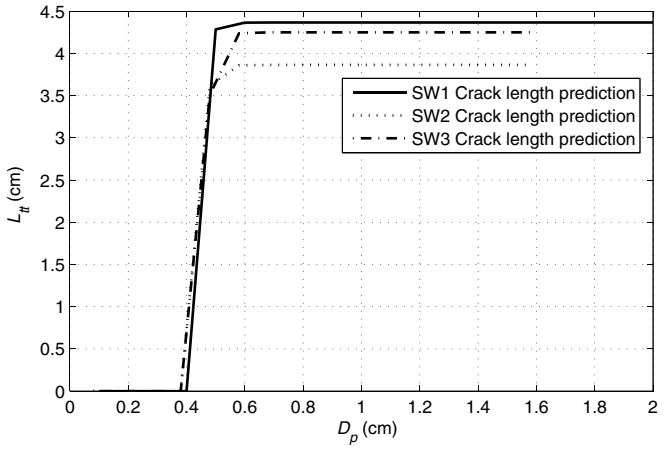

Fig. 9. Crack length prediction with W-S equation ($V = 3$ km/s, 0° impact angle).

manned spacecraft under different debris diameters and impact velocities, as shown in Eqs. 14 and 15. Since only perforation data under an impact velocity of 3 ± 0.2 km/s were obtained from impact tests, only the coefficients F_p and F_S in the perforation equation for region 1 were modified, and the perforation equations for regions 2 and 3 and the crack length equation remain are consistent with those in the study of Williamsen and Schonberg [18] in terms of form and coefficients.

$$D_h = A_h\left(\frac{V}{6.5}\right)\cos^{B_h}\theta_p\left\{1-exp\left[-C_h\left(\frac{D_p}{D_{BL}}-1\right)\right]\right\} \quad (14)$$

$$L_{tt} = A_L\left(\frac{V}{6.5}\right)\cos^{B_L}\theta_p\left\{1-exp\left[-C_L\left(\frac{D_p}{D_{BL}}-1\right)\right]\right\} \quad (15)$$

In the case of impact angles $\theta_p > 65^\circ$ and $\theta_p = 65^\circ$

$$A_h = 3F_S\max\left(F_T, F_p\right).$$

$B_h = -0.5\left(V_B - 11\right)\left(1-\rho_{IB}^{AD}/0.79\right)$; if $B_h < 0$, then $B_h = 0$; $C_h = 2\max\left(F_T, F_p\right)$.

$A_L = 6F_S\left(\sigma_y^w/393\right)\max\left(F_T, F_p\right)$, $B_L = B_h$, and $C_L = 2F_P\left(V_C/6.5\right)^2\left(393/\sigma_y^w\right)\sqrt{F_S}$.

$F_T = 0.478/t_w$; if $F_T < 1$, then $F_T = 1$;

$F_p = 2\left[\frac{S-S_2}{S}\right]\sqrt{\frac{\rho_{IB}^{AD}+\rho_w^{AD}}{\rho_w^{AD}}}$; if $F_p < 1$, then $F_p = 1$; $F_S = 1$;

V_B should be determined as follows:

$$V_B = \left\{\begin{array}{ll} 6.5\ \text{km/s} & , V < 6.5\ \text{km/s} \\ V_P & , 6.5\ \text{km/s} \le V \le 11\ \text{km/s} \\ 11\ \text{km/s} & , V < 11\ \text{km/s} \end{array}\right\}.$$

where D_h is the perforation diameter on the sealed cabin wall, L_{tt} is the crack length on the sealed cabin wall, D_p is the projectile diameter, S_2 is the distance from the rear wall of the stuffing layer to the sealed cabin wall, ρ_{IB}^{AD} and ρ_w^{AD} are the areal densities of the stuffing layer and the cabin wall, respectively, and σ_y^w is the yield stress of the cabin wall material. V_C is determined in the same way as V_B. Other parameters have the same meanings as the abovementioned.

Depending on the structural parameters of 3 types of shield structures for a specific ultralarge manned spacecraft and the modified perforation and crack equations, perforation diameter and crack length on the sealed cabin under an impact velocity of 3 km/s and an impact angle of 0° were predicted (Figs. 8 and 9).

It should be noted that, limited by the amount of test data and the particularity of the test object, the modified limit equation and perforation equation are only applicable to the filled protective structure of a large manned spacecraft in China.

Downloaded from https://spj.science.org on October 20, 2023

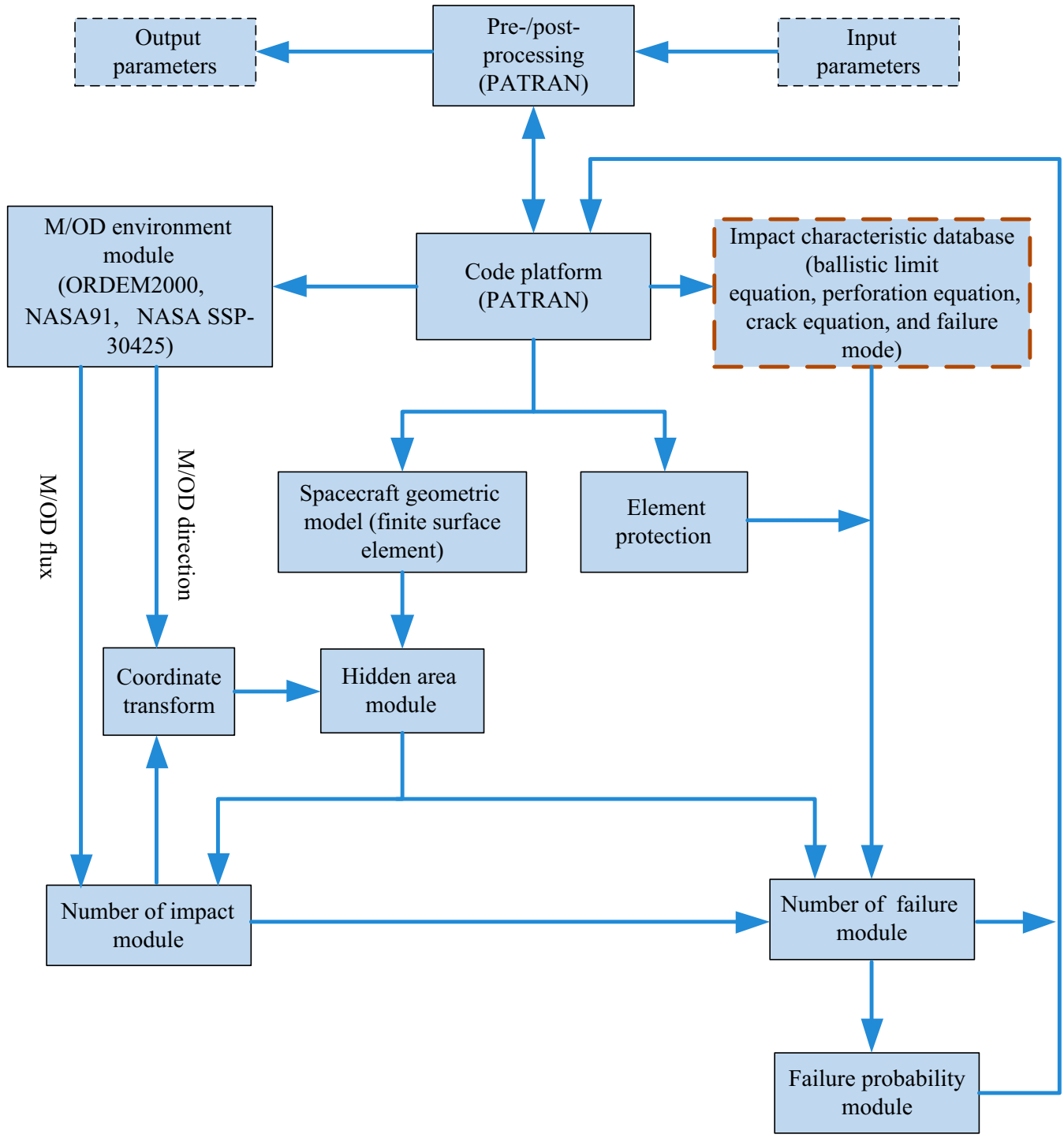

Fig. 10. MODAOST evaluation software framework.

Catastrophic Failure Assessment of Sealed Cabin of Ultralarge Manned Spacecraft in M/OD Environment

Assessment module integration based on MODAOST framework

MODAOST developed by the China Academy of Space Technology has the functions of assessing and optimizing the protection capabilities of on-orbit spacecraft such as M/OD impact probability and penetration probability and has been successfully used for on-orbit PNP assessment of manned spacecraft of multiple models, such as the Tiangong-1 space module and the Tianhe core module [1,2,6]. The main functional modules of MODAOST are shown in Fig. 10. Among these modules, the impact characteristic database is used to describe failure modes of spacecraft and corresponding failure models. On the basis of the current software, the impact characteristic database was expanded by adding the database modules of ballistic limit equations, perforation diameter calculation, and crack length calculation, as well as corresponding failure criterion modules

Downloaded from https://spj.science.org on October 20, 2023

Table. M/OD risk assessment of ultralarge manned spacecraft assembly (1 year).

Particle source / Failure mode		Orbital debris	Micrometeoroid	M/OD
Penetration	*PP*	2.76930×10^{-3}	2.24039×10^{-4}	2.9933×10^{-3}
	PNP	9.97231×10^{-1}	9.99776×10^{-1}	9.97007×10^{-1}
Breakup	*PNCF*	9.99916×10^{-1}	9.99996×10^{-1}	9.99996×10^{-1}
	R	3.03326×10^{-2}	1.78540×10^{-2}	1.33630×10^{-3}
Sealed cabin fracture	*PNCF*	9.99946×10^{-1}	9.99990×10^{-1}	9.99935×10^{-1}
	R	1.94995×10^{-2}	4.46351×10^{-2}	2.17149×10^{-2}
Astronaut hypoxia	*PNCF*	9.99575×10^{-1}	9.99949×10^{-1}	9.99524×10^{-1}
	R	1.53468×10^{-1}	2.27639×10^{-1}	1.59020×10^{-1}

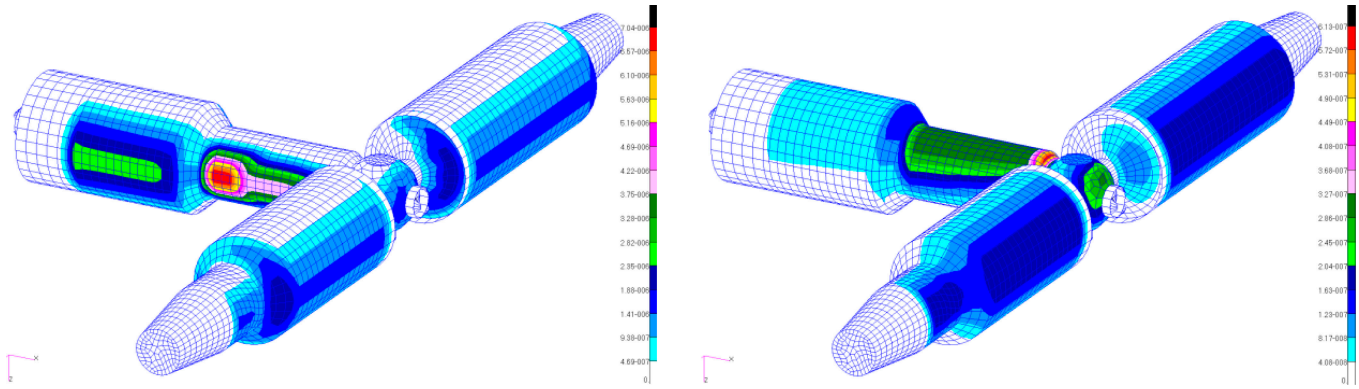

A Perforation number of orbital debris

B Perforation number of micrometeoroid

Fig. 11. Perforation number of orbital debris (A) and micrometeoroid (B).

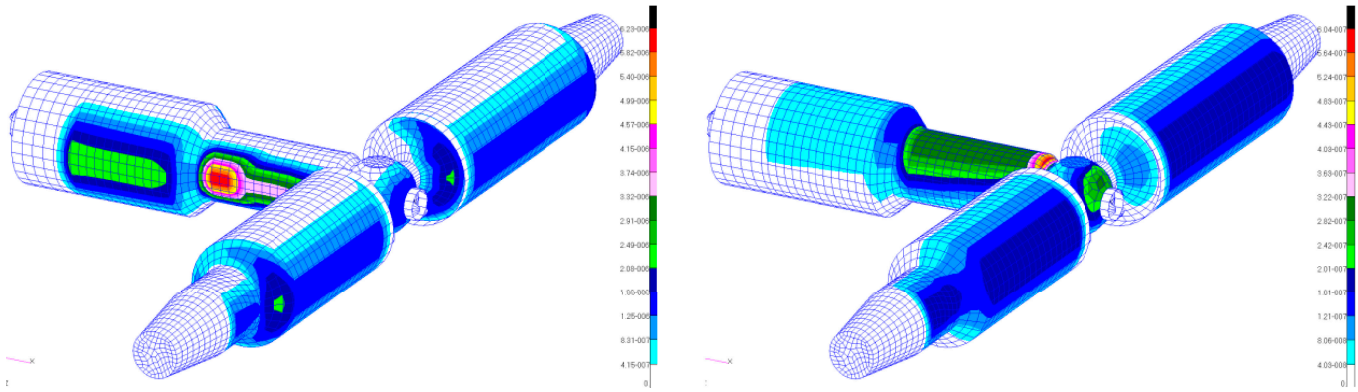

A Perforation number of orbital debris causing astronaut hypoxia

B Perforation number of micrometeoroid causing astronaut hypoxia

Fig. 12. Perforation number of orbital debris (A) and micrometeoroid (B) causing astronaut hypoxia.

of the sealed cabin structure that were supplemented. In this way, MODAOST has the functions of risk assessment under the typical catastrophic failure modes such as gas-leakage-induced astronaut hypoxia, sealed cabin fracture, and breakup of manned spacecraft.

The critical perforation diameter was calculated in the impact characteristic database and then used as the criterion for the astronaut hypoxia failure mode. Regarding M/OD with different sizes, directions, and velocities and corresponding impact probabilities, we can assess this impact event just by calculating the perforation diameter and comparing it with the criterion. Compared with the Monte Carlo method used by MSCSurv, which needs to calculate escape time under the impact for each impacting debris particle and then compare it with the critical escape time [4], the calculation and evaluation efficiency are greatly improved.

Downloaded from https://spj.science.org on October 20, 2023

During assessment of astronaut hypoxia mode, to simplify the evaluation process, other factors that affect the safety of astronauts were ignored, such as the position of the astronauts at this time, their current working or living conditions, the opening and closing state of the hatch, and other effects caused by the impact event. In addition, the state of the manned spacecraft used for the emergency escape of astronauts was unconsidered.

Verification of catastrophic failure assessment of ultralarge manned spacecraft

The 3-module assembly of a specific ultralarge manned spacecraft had an orbit of 400 km and an orbit inclination of 42°, flying in a triaxial stable attitude. The stuffed Whipple shields were adopted for the whole sealed cabin. The sealed cabin has a volume of 100 m^3, containing a mixture of nitrogen and oxygen with respective proportions of 79% and 21%. The gas temperature is 21 °C, and the internal pressure is 1.01×10^5 Pa. The total pressure for emergency leakage plugging or evacuation is 70 kPa, and the oxygen partial pressure is 14 kPa.

The Grün model and ORDEM2000 are used for M/OD environment modeling. On this basis, M/OD impact risks of the assembly during its 1-year on-orbit operation are assessed (Table and Figs. 11 and 12).

Among the typical failure modes, the gas-leakage-induced astronaut hypoxia is the primary factor, with the R factor reaching 0.159. Compared with the PNP assess method, the PNCF of the system achieved by the proposed method increases from 0.9970 to 0.9995, followed by the sealed cabin fracture, while spacecraft breakup is of the lowest probability. Under orbital debris impact, quadrants II and IV of the small column segment of the core module are the riskiest zones of perforation failure, while quadrant III of the small column segment is the riskiest zone under micrometeoroid impact.

Conclusion

Typical catastrophic failure modes of manned spacecraft include gas-leakage-induced astronaut hypoxia, sealed cabin fracture, and spacecraft breakup. In view of these failure modes, this paper proposes catastrophic failure assessment based on critical perforation diameter and CCL of sealed cabins and critical fragment size of spacecraft breakup. In addition, catastrophic failure assessment modules for manned spacecraft in an M/OD environment are developed to extend the functions of MODAOST. On this basis, catastrophic failure risk assessment software is formed with a simple framework, fast calculation, and efficient assessment, thus providing an effective support tool for studying catastrophic failures of ultralarge manned spacecraft in an M/OD environment. This paper also establishes ballistic limit equations of the stuffed Whipple shield of a specific ultralarge manned spacecraft as well as the perforation and crack equations of the sealed cabin. Further, the paper quantitatively assesses the catastrophic failures of a specific ultralarge manned spacecraft in an M/OD environment using MODAOST, providing reference for the design and assessment of long-term on-orbit missions of the spacecraft.

Acknowledgments

Funding: We would like to acknowledge the support of National Great Science and Technology special project for this work.

Author contributions: J.W. was responsible for overall coordination, simulations, and paper writing. Z.H. and Y.Z. proposed the original idea and the access framework. R.C. performed the analysis of the test data. S.Z. was responsible for the experiment and offered many valuable helps and suggestions. **Competing interests:** The authors declare that they have no competing interests.

Data Availability

The data used to support the findings of this study are available from the corresponding author upon reasonable request.

References

1. Jun Y, Shigui Z, Wei Y, Weiwei G. Space debris protection design for the space station. *Space Debris Res*. 2021;21(2):1–9 (in Chinese).
2. Jun Y, Zheng S, Zengyao H, Yang L. Space debris protection design and application for Tiangong-1. *Scientia Sinica(Technologica)*. 2013;43(5):478–486 (in Chinese).
3. Pernigoni L, Lafont U, Grande AM. Self-healing materials for space applications: Overview of present development and major limitations. *CEAS Space J*. 2021;13:341–352.
4. Graves R. Space Station meteoroid and orbital debris survivability. Paper presented at: 43rd Structure, Structural Dynamics and Materials Conference; 2002; Houston, TX.
5. Williamsen J, Evans H, Bohl B. Quantifying and improving International Space Station survivability following orbital debris penetration. Paper presented at: 52nd International Astronautical Congress; 2001; Toulouse, France.
6. Zengyao H, Zheng S, Jun Y, Jingyan F, Guangji Q. Development, calibration and application of space debris impact probability analysis software. *J Astronaut*. 2005;26(2):228–231 (in Chinese).
7. Weibo L, Zhaoxia L, Jindun C, Yuankai P. Selection of spacecraft atmospheric pressure regime for manned lunar exploration mission. *Manned Spaceflight*. 2016;22(6):687–693 (in Chinese).
8. Wang D, Peng Z. Non-steady-state gas leakage model for pressure vessel failure. *China Safety Sci J*. 2012;07(22):154–160 (in Chinese).
9. Jian J, Yang C, Yongqing H. Simulation model for air pressure control system of manned spacecraft. *Spacecraft Eng*. 2015;24:51–57 (in Chinese).
10. Lutz B, Williamsen J. Critical fracture of Space Station modules following orbital debris penetration. *Br J Pharmacol*. 2013;136(7):985–994.
11. Lutz BEP, Goodwin CJ. Catastrophic failure modes assessment of the International Space Station Alpha. NASA Contractor Report 4720; 1996.
12. Yi L, Jie H, Zhaoxia M, Shengwei L, Sen L. A new breakup threshold model for satellite under hypervelocity impact. *J Astronaut*. 2012;33(8):1158–1163.
13. Williamsen JE. Vulnerability of manned spacecraft to crew loss from orbital debris penetration. NASA TM-108452; 1994.
14. Zheng S, Gong W, Yan J. Impact Characterization of Stuffed Whipple for China Space Station. Paper presented at: 7th European Conference on Space Debris; 2017; Darmstadt, Germany.
15. Ryan S, Christiansen EL. Micrometeoroid and Orbital Debris (M/OD) Shield Ballistic Limit Analysis Program: NASA JSC. NASA JSC TM-2009-214789; 2009.

Downloaded from https://spj.science.org on October 20, 2023

16. Williamsen JE, Schonberg WP, Evans HJ. Spacecraft module hole size and crack length prediction following a penetrating debris particle impact. *Procedia Engineering*. 2013;58:11–20.
17. Wu J, Chi R, Sun G, Han Z, Pang B, Zheng S. Experiment study on the impact limit of basalt/aramid stuffed whipple shields. In: Sun J, Wang Y, Huo M, Xu L. editors. *Signal and information processing, networking and computers*. Lecture Notes in Electrical Engineering. Singapore: Springer; 2023. vol. 917. https://doi.org/10.1007/978-981-19-3387-5_24
18. Williamsen J, Schonberg W. An Improved Prediction Model for Spacecraft Damage Following Orbital Debris Impact. Paper presented at: AIAA/ASME/ASCE/AHS/ASC Structures, Structural Dynamics & Materials Conference AIAA/ASME/AHS Adaptive Structures Conference AIAA; 2006 Apr 23–26; Honolulu, Hawaii.

Downloaded from https://spj.science.org on October 20, 2023